HHS Public Access

Author manuscript

J Magn Reson Imaging. Author manuscript; available in PMC 2017 November 01.

Published in final edited form as:

J Magn Reson Imaging. 2016 November ; 44(5): 1312–1319. doi:10.1002/jmri.25252.

Quantification of Renal Steatosis in Type II Diabetes Mellitus using Dixon-Based Magnetic Resonance Imaging

Takeshi Yokoo, MD PhD[1,2], **Haley R Clark, MD**[1], **Ivan Pedrosa, MD**[1,2], **Qing Yuan, PhD**[1], **Ivan Dimitrov, PhD**[2,6], **Yue Zhang, PhD**[1], **Ildiko Lingvay, MD**[3,4], **Muhammad S Beg, MD**[3], and **I Alexandru Bobulescu, MD**[3,5]

[1]Department of Radiology, University of Texas Southwestern Medical Center, Dallas, TX USA

[2]Advanced Imaging Research Center, University of Texas Southwestern Medical Center, Dallas, TX USA

[3]Department of Internal Medicine, University of Texas Southwestern Medical Center, Dallas, TX USA

[4]Department of Clinical Science, University of Texas Southwestern Medical Center, Dallas, TX USA

[5]Charles and Jane Pak Center of Mineral Metabolism and Clinical Research, University of Texas Southwestern Medical Center, Dallas, TX USA

[6]Philips Medical Systems, Cleveland, OH USA

Abstract

Purpose—To evaluate renal lipid content in subjects with and without type II diabetes mellitus (DM2) using Dixon-based magnetic resonance imaging (MRI).

Materials and Methods—This retrospective study was approved by institutional review board and compliant with Health Insurance Portability and Accountability Act. Sixty-nine adults with or without DM2 (n=29, n=40) underwent 3T MRI of the abdomen using 3D multiecho Dixon gradient-echo acquisition and proton-density fat fraction (FF) reconstruction. FF values were recorded within segmented regions of interest in the kidneys and liver. The FF measurement error was estimated from the within-subject difference between the right and left kidneys using Bland-Altman Analysis. Correlation between renal FF, hepatic FF, and body mass index (BMI) was evaluated. The association between renal FF and DM2 was evaluated by Wilcoxon rank sum test as well as by multivariate regression to correct for potential confounding effects of age, sex, BMI, creatinine, and hepatic FF. P-values <0.05 were considered statistically significant.

Results—Per-subject 95% limit of agreement of the renal FF measurement was [−3.26%, +3.22%]. BMI was significantly correlated to renal FF (r=0.266, p=0.027) and to liver FF (r=0.344, p=0.006). Correlation between renal and hepatic FF did not reach statistical significance (r=0.215, p=0.090). Median renal FF (±interquartile range) was 2.18% (±2.52%) in the DM2 cohort, significantly higher than 0.80% (±2.63%) in the non-DM2 cohort (p<0.001). After

Corresponding Author Info, Takeshi Yokoo, M.D. Ph.D., University of Texas Southwestern Medical Center, 2201 Inwood Road, NE2.210B, Dallas, TX, USA 75390-9085, Takeshi.Yokoo@UTSouthwestern.edu, 214-645-2715 (voice), 214-645-2762 (fax).

correcting for potential confounders, the relationship between DM2 and renal FF remained statistically significant (p=0.005).

Conclusion—Renal lipid content can be measured noninvasively using Dixon-based MRI and may be increased in subjects with DM2 compared to those without DM2.

Keywords

Renal steatosis; diabetes; obesity; chronic kidney disease; proton-density fat fraction; Dixon technique

INTRODUCTION

Obesity, type II diabetes mellitus (DM2), and metabolic syndrome are major independent risk factors of chronic kidney disease (CKD) and end-stage renal disease (ESRD) (1-3). While the pathogenic mechanisms linking these metabolic disorders with kidney disease are not fully understood, a growing body of evidence suggests that renal lipid accumulation (renal steatosis) and the deleterious effects of excess lipids (lipotoxicity) contribute to the pathogenesis and progression of CKD (4,5). However, existing lines of evidence have been derived primarily from animal models, and their applicability to humans remains uncertain. Further research in humans is critically important, but to date has been hampered by the lack of a reliable, noninvasive method of renal lipid measurement in a clinical setting.

Direct histochemical staining (e.g. oil-red-O) or biochemical measurement of triglycerides in the renal tissue remains the gold-standard methods for evaluating renal steatosis (6-8). However, utilization of renal biopsy for clinical care and research has been limited due to procedure risk and ethical considerations. Recently, quantitative magnetic resonance imaging (MRI) and spectroscopy (MRS) techniques have been introduced for noninvasive measurement of tissue proton-density fat fraction (FF) (9). Initially developed as a noninvasive biomarker for hepatic steatosis, these techniques have subsequently been applied to measure lipid content in the pancreas, bone marrow, and skeletal muscle (10-15). In the kidney, animal studies have shown renal lipid accumulation in rodent models of DM2 using histochemical and/or biochemical analysis (16-18) as well as ultrahigh-field MRI (19). Studies of healthy volunteers using 1.5T MRI and MRS demonstrated that normal human kidneys have very low lipid content, approximately 0.4-0.7% in FF (20,21). However, lipid accumulation in human kidneys has not yet been demonstrated using clinical-field (≤3T) MRI or MRS.

Therefore, the purpose of this study was to evaluate the clinical feasibility of noninvasive renal lipid measurement using Dixon-based MRI and to determine whether renal lipid accumulation is associated with obesity and DM2.

MATERIALS AND METHODS

Study Design and Patient Population

This pilot study was a retrospective analysis of prospectively acquired data obtained from three clinical research studies conducted at a single institution. Each study was approved by

the local institutional review board and compliant with the Health Insurance Portability and Accountability Act. A written informed consent was obtained from each subject prior to study participation. An additional IRB approval with waiver of informed consent was obtained for present retrospective analysis. Study 1 consisted of 40 subjects with suspected or known renal cancer with planned surgical nephrectomy. Study 2 consisted of 10 subjects with known locally advanced or metastatic pancreatic cancer. Study 3 consisted of 19 subjects with known insulin-dependent DM2. In each study, subjects underwent baseline MRI of the abdomen including the kidneys prior to the study-specific intervention, if any. The detailed inclusion/exclusion criteria are summarized in Table 1. By electronic chart review, age, sex, body mass index (BMI) and history of DM2 were recorded, as well as contemporaneous serum creatinine and hemoglobin A1c (HbA1c, if available) within 3 months prior to the baseline MRI.

MRI Examination

All MRI exams were performed using 3T whole-body systems (Achieva or Ingenia, Philips Healthcare, Best, the Netherlands) using a 16- or 28-channel phased-array torso receive coil, respectively. Each exam included localizing coronal and axial T2-weighted single-shot fast spin-echo sequences as well as axial 3-D multiecho Dixon gradient-recalled echo sequence (mDixon-Quant) acquired within a 22-s or less breath-hold (22), with automatic reconstruction of proton-density fat fraction (FF) maps (23,24). The acquisition volume was centered in the renal masses (study 1) or the pancreas (study 2 and 3) with at least upper pole of the kidneys included. The axial section thickness was 6-, 5-, and 4-mm for study 1, 2, and 3, respectively. Six TEs (first TE 0.9-1.2 ms, ΔTE 0.9-1.1 ms) were acquired using TR 6.7-8.0 ms, flip angle 2-3°, default parallel imaging SENSE factor 2 (if phased-array coil and parallel imaging used), and Number of Signal Average 1. The matrix size 228-280 × 180-210, field-of-view (FOV), and number of slices, were adjusted to accommodate subjects' body habitus and breath-hold capacity. In morbidly obese subjects not permitting the placement of a phased-array coil, a built-in body coil was used without SENSE, reducing the number of slices by a factor of 2. In addition, when obvious SENSE fold-over artifact was encountered in the center of FOV, SENSE was turned off to remove this artifact. One subject in Study 1 was scanned with TR 16 ms but otherwise standard imaging parameters; this subject was included in the study, as longer TR (i.e. less T1-weighting) is not expected to bias the FF measurement.

Image Analysis

All image analysis was performed on anonymized data using a picture archiving and communication system (OsiriX, Pixmeo, Bernax, Switzerland) by investigators blinded to the demographic and clinical data, except for visually obvious obesity status or presence of a renal or pancreatic mass. Under the supervision of a fellowship-trained abdominal radiologist (TY, 9-year experience), a radiology resident (HRC, 2-year experience) selected a representative section through each kidney and manually segmented the renal parenchyma using a free-hand region-of-interest (ROI) tool. No attempt was made to separately segment cortex and medulla, as the boundaries were not clearly seen in all subjects. Attention was paid to avoid possible areas of artifacts such as the boundaries along the perinephric or renal sinus fat, as well as benign renal lesions such as cysts (as seen on the accompanying T2-

weighted images). In patients with renal cancer, analysis was done only in the non-tumor-bearing kidney. In the portion of the right hepatic lobe included in the imaged volume, a largest ROI was manually segmented, avoiding visible intrahepatic vessels, bile ducts, and areas of imaging artifacts. In the included portion of the spleen, a manually segmented ROI was placed in a similar fashion. Typical ROI placements are illustrated in Figure 1. For each ROI, the mean FF and the area (cm^2) were recorded.

Statistical Analysis

Statistical analyses were performed by one author (TY, >10 years experience) using MATLAB statistical toolbox (Mathworks, Natick, MA). To assess the consistency of renal lipid measurement, the right and left renal FF values were compared in whom both renal measurements were made, using linear regression analysis, a paired *t*-test, and Bland-Altman Analysis. The 95% limit of agreement was calculated to estimate the FF measurement error. The demographic, clinical, laboratory, and FF data were tabulated and summarized according to the DM2 status. Differences between the non-DM2 and DM2 cohorts were analyzed using univariate analyses: χ^2 test for categorical data (sex) and Wilcoxon rank sum test for quantitative data (age, BMI, creatinine, hepatic, renal, and splenic FF). Pearson's linear correlation analysis was used to assess the relationship between renal FF, hepatic FF, and BMI. Similarly, the correlation of renal FF with creatinine and HbA1c was assessed. For HbA1c, the correlation was calculated only in the DM2 subjects using their available HbA1c data. To examine the unconfounded effect of DM2, renal FF (the response variable) was modeled using a multiple linear regression model with age, sex, BMI, DM2, creatinine, and hepatic FF as predictor variables. P-values < 0.05 were considered statistically significant.

RESULTS

Of the 69 subjects pooled from three studies, 29 subjects had history of DM2 (8, 2, 19 subjects from Study 1, 2, 3, respectively), and 40 did not (32, 8, 0, subjects from Study 1, 2, 3 respectively). No subject had type I diabetes. Fifty-four (n=54; 25 with DM2) subjects were imaged on the Achieva and fifteen (n=15; 4 with DM2) on the Ingenia platform. Seven (n=7) of the DM2 subjects were too large to be imaged on the Achieva platform (60 cm bore diameter) using phased-array coil and therefore were imaged with the built-in body coil. A phased-array coil was used for all subjects imaged on the Ingenia platform (70 cm bore diameter). SENSE parallel imaging was used in 17 DM2 subjects and 17 non-DM2 subjects. In all subjects, at least upper portions of both kidneys were included in the mDixon-Quant acquisition. The acquired volume did not include liver in 5 subjects and spleen in 12 subjects. The mean ROI size ± SD in the right and left kidneys were 8.86 ± 2.69 cm^2 and 9.50 ± 3.14 cm^2, respectively, liver 31.42 ± 16.60 cm^2, and spleen 15.80 ± 9.24 cm^2.

The demographic, clinical, laboratory, and FF data of the study population are summarized in Table 2. The BMI, hepatic FF, renal FF, and splenic FF values of the non-DM2 and DM2 cohorts are graphically presented in Figure 2. Statistically significant differences between the two cohorts were found in BMI, hepatic and renal FF values, all three being higher in the DM2 cohorts. No significant difference was found in the splenic FF between the diabetics and non-diabetics.

In 29 subjects with FF measurements in both kidneys (i.e. in studies 2 & 3), no significant differences were found between the two kidneys in terms of linear regression slope and intercept estimates (Figure 3A) or by paired *t*-test (p = 0.947). The mean right-left FF difference was 0.021% with standard deviation 1.655%. The 95% limit of agreement was [−3.264, +3.223]%, representing an estimate of the measurement precision of this method. Figures 3B and 3C show modest but significant correlation between renal FF and BMI as well as hepatic FF and BMI. However, the correlation between renal and hepatic FF values did not reach statistical significance (Figure 2D). No significant correlation was found between renal FF and serum creatinine (Figure 4A) or HbA1c in the DM2-cohort (Figure 4B). Multiple linear regression analysis (Table 3) shows that DM2 is independently associated with elevated renal FF even after correction for the effects of age, sex, BMI, creatinine, and hepatic FF.

DISCUSSION

The normal triglyceride content in the human kidney is estimated to be 0.6% by wet weight (5,26). Abnormal renal accumulation of triglycerides, or renal steatosis, has been found in a number of animal models of obesity, diabetes, and metabolic syndrome, and is thought to be a marker of lipotoxic kidney dysfunction (5,27). There is a need to translate these findings to the human kidney. However, the need for histochemical examination and/or biochemical lipid assays of renal tissue has thus far limited the study designs to include only a small number of patients undergoing surgery or biopsy for clinical care (6,7). Given the invasive nature of tissue-based methods, noninvasive methods are needed for further research.

MRI and MRS, due to their chemical specificity for triglycerides, hold great promise as a potential research tool for human renal steatosis. Our pilot study supports the feasibility of noninvasive measurement of renal lipid content using Dixon-based MRI at clinical field-strengths. Furthermore, increased renal lipid content measured by MRI was associated with DM2, independent of BMI. This association with DM2 is consistent with histological and biochemical findings in previous human (7,28) and animal studies (16-18). Our findings are also in agreement with a recent ultrahigh-field (7T) animal study demonstrating higher renal FF in diabetic db/db mice compared to control mice (19).

Other notable findings of this study and their implications are as follows. First, renal FF had moderate-correlation with obesity as measured by BMI, as previously suggested based on biochemical triglyceride content in nephrectomy specimens (6). However, as BMI was not a significant factor in our multivariate analysis, this correlation could be spurious due to the correlation between BMI and DM2. This observation is also in agreement with a recent clinical field (1.5T) MRI study that did not find correlation between renal FF and BMI in healthy non-diabetic volunteers (21). Second, human kidneys appear to be very low in lipid content. In our study, the median renal FF in non-DM2 cohort was 0.82%, in close agreement with the literature value of 0.6% and consistent with prior human volunteer studies using MR imaging (21) and spectroscopy (20,29). Even in the DM2 cohorts, the median renal FF value was only 2.38%. These findings are also consistent with the low level of triglycerides and approximately 3-fold range observed in a previous analysis of the obesity-related renal steatosis in the biochemical analysis of surgical specimen (6). This low

and small range of renal FF is in contradistinction to hepatic FF whose upper limit of normal is approximately 6% (30,31) and in pathologic cases can reach above 40%. Despite this relatively narrow range, even small elevations in renal lipid content may be pathophysiologically significant, as the kidney is not normally a lipid storage organ, unlike the liver (5). Third, we did not find statistically significant correlation between the renal FF to creatinine or HbA1c (latter in the DM2 cohort only). However, these results are likely biased due to the retrospective design. Specifically, the creatinine data is confounded by (a) exclusion of subjects with abnormal serum creatinine in Study 1 and (b) underlining cancer potentially impacting the creatinine in subjects in Studies 1 and 2. The HbA1c data is confounded as the majority of the DM2 subjects were pre-selected to have uncontrolled DM2 with HbA1c range of 7.5 – 11% in Study 3. Lastly, we did not find statistically significant correlation between the hepatic and renal FF, despite both being higher in the DM2 cohorts. While this is consistent with another MRI study comparing hepatic and renal FF (21), several other non-imaging studies have shown a link between nonalcoholic fatty liver disease (NAFLD) and CKD (32,33). The pathogenesis of steatosis in liver and kidney are fundamentally different so it is conceivable that there may be discordance in specific metabolic conditions. Due to relatively small sample size, this pilot study is likely under-powered to conclude lack of correlation between renal and hepatic steatosis. With increasing use of MRI or MRS in metabolic kidney diseases, the relationship between hepatic steatosis, renal steatosis, and renal dysfunction may be elucidated in the future.

A major strength of this study is the use of proton-density FF, an existing MR biomarker of steatosis, extensively validated in the liver in the setting of NAFLD (34-36). The Dixon-based pulse sequence used, mDixon-Quant, is commercially available and is approved by the Food and Drug Administration for the liver triglyceride quantification by MRI. Similar techniques have been applied to other organs, such as pancreas, bone marrow, and skeletal muscle as steatosis biomarkers in the respective organs (10-15). For lipid measurement in the kidneys, MRI has some advantages over MRS, including the breath-hold acquisition and precise intra-renal placement of ROI, thereby obviating precise respiratory motion compensation needed for spectroscopy and avoiding the contamination by the perinephric and renal sinus bulk fat. Imaging also has a unique potential (though not performed in this study) of differentiating the renal cortex from the medulla, and FF can be measured separately in these anatomically and functionally distinct compartments. As lipid may accumulate preferentially in the glomeruli and proximal tubules (5,6), cortex-specific FF measurement, made possible by imaging, may be worth future investigation.

This pilot study has several limitations. Selection bias is inherent to the study's retrospective design; the non-DM2 cohort was comprised of cancer patients without DM2 rather than normal healthy volunteers. While no specific association between cancer and renal steatosis is currently known, the impact of cancer on renal lipid metabolism in humans is not known, and a potential confounding effect cannot be excluded. The ROI placement in the kidneys was not standardized across the pooled study population, as the anatomical coverage was different in the three studies; study 1 was centered at the renal masses, whereas study 2 and 3 were centered at the pancreas, often resulting in partial renal coverage. Liver and spleen data were available for most, but not all subjects, as the liver and spleen coverage was also variable. We employed a segmentation approach to ROI selection to overcome the effect of

local heterogeneity of steatosis, if present. Since DM2 is a systemic metabolic disease, it is likely to affect both kidneys equally. The agreement between the right and left renal FF measurements suggest, albeit indirectly, independence of the ROI location within the kidneys. The slice thickness (6-, 5-, and 4-mm) and scanner model (Philips Achieva and Ingenia) were similarly not standardized. Differences in slice thickness, SENSE factor, and receiver coil selection, may affect signal-to-noise ratio (SNR) of the source images and could influence the pixel-by-pixel FF estimates. The mDixon-Quant reconstruction algorithm employs noise-bias correction (37) to increase estimation robustness under varying SNR. Also, averaging over large number of pixels in segmented ROIs should have mitigated the effect of FF estimation noise. The lack of significant difference in the splenic FF supports the notion that slice thickness likely did not contribute to the effect seen for renal FF. Though not directly confirmed in this study, the difference in scanner models also is not expected to impact proton-density FF estimates based on previous multi-vendor, multi-platform reproducibility studies of hepatic steatosis (38,39). Lastly, the observed effect size (i.e. the difference FF between the DM2 and non-DM2 cohorts) was 1.56%, small in comparison to the inherent measurement SD of 1.66%. While this effect size was statistically detectable at the group level, such small differences would be difficult to detect on a per-subject basis. Certain technical parameters may impact the measurement precision, including field strengths, receiver coils, 3D vs.2D acquisition, slice thickness, parallel imaging, and the details of PDFF estimating algorithms (e.g. complex or magnitude), but these effects were not systematically investigated in this study. While previously reported high reproducibility across different PDFF protocols designed for liver imaging (38,39) is promising for general applicability in the kidneys, different optimization strategies may be needed for kidney imaging. For these reasons, our study findings need to be validated in a carefully controlled prospective study with an optimized protocol, which is ongoing at our institution.

In conclusion, this pilot retrospective study found increased renal lipid in subjects with type II diabetes compared to those without diabetes using Dixon-based MRI at 3T. The potential utility of renal lipid measurement by MRI as a non-invasive biomarker of chronic kidney disease requires further prospective validation.

Acknowledgement

We would like to thank the following individuals: Orson W Moe, MD and Robert E Lenkinski, PhD, for inspiring this study and providing valuable input throughout the manuscript preparation; Jeremy Warshauer, MD, and Debbie Travalini, PA-C, for their help collecting clinical data; Trevor Wigal, RT, and Shiju Varughese, RT for MR data acquisition; Christina Carrigan, RN, and Radiology Clinical Research Office for their logistical support.

Grant Support

IP was in part supported by NIH grant NCI 1R01CA154475

IL was in part supported by Investigator Initiated Trial Grant from NovoNordisk

MSB was in part supported by ACS grant IRG-02-196-10 and NIH grant NCATS UL1TR001105

IAB was in part supported by NIH grant NIDDK K01-DK090282

REFERENCES

1. Mathew AV, Okada S, Sharma K. Obesity related kidney disease. Current diabetes reviews. 2011; 7(1):41–49. [PubMed: 21067508]
2. Williams ME. Diabetic CKD/ESRD 2010: a progress report? Seminars in dialysis. 2010; 23(2):129–133. [PubMed: 20210917]
3. Whaley-Connell A, Sowers JR, McCullough PA, et al. Diabetes mellitus and CKD awareness: the Kidney Early Evaluation Program (KEEP) and National Health and Nutrition Examination Survey (NHANES). American journal of kidney diseases : the official journal of the National Kidney Foundation. 2009; 53(4 Suppl 4):S11–21. [PubMed: 19285607]
4. Zhang X, Li ZL, Woollard JR, et al. Obesity-metabolic derangement preserves hemodynamics but promotes intrarenal adiposity and macrophage infiltration in swine renovascular disease. American journal of physiology Renal physiology. 2013; 305(3):F265–276. [PubMed: 23657852]
5. Bobulescu IA. Renal lipid metabolism and lipotoxicity. Current opinion in nephrology and hypertension. 2010; 19(4):393–402. [PubMed: 20489613]
6. Bobulescu IA, Lotan Y, Zhang J, et al. Triglycerides in the human kidney cortex: relationship with body size. PloS one. 2014; 9(8):e101285. [PubMed: 25170827]
7. Herman-Edelstein M, Scherzer P, Tobar A, Levi M, Gafter U. Altered renal lipid metabolism and renal lipid accumulation in human diabetic nephropathy. Journal of lipid research. 2014; 55(3):561–572. [PubMed: 24371263]
8. Nielsen H, Thomsen JL, Kristensen IB, Ottosen PD. Accumulation of triglycerides in the proximal tubule of the kidney in diabetic coma. Pathology. 2003; 35(4):305–310. [PubMed: 12959765]
9. Reeder SB, Hu HH, Sirlin CB. Proton density fat-fraction: a standardized MR-based biomarker of tissue fat concentration. Journal of magnetic resonance imaging : JMRI. 2012; 36(5):1011–1014. [PubMed: 22777847]
10. Idilman IS, Tuzun A, Savas B, et al. Quantification of liver, pancreas, kidney, and vertebral body MRI-PDFF in non-alcoholic fatty liver disease. Abdominal imaging. 2015; 40(6):1512–1519. [PubMed: 25715922]
11. Kuhn JP, Berthold F, Mayerle J, et al. Pancreatic Steatosis Demonstrated at MR Imaging in the General Population: Clinical Relevance. Radiology. 2015; 276(1):129–136. [PubMed: 25658037]
12. Kuhn JP, Hernando D, Meffert PJ, et al. Proton-density fat fraction and simultaneous R2* estimation as an MRI tool for assessment of osteoporosis. European radiology. 2013; 23(12):3432–3439. [PubMed: 23812246]
13. Patel NS, Peterson MR, Lin GY, et al. Insulin Resistance Increases MRI-Estimated Pancreatic Fat in Nonalcoholic Fatty Liver Disease and Normal Controls. Gastroenterology research and practice. 2013; 2013:498296. [PubMed: 24348536]
14. Baum T, Yap SP, Dieckmeyer M, et al. Assessment of whole spine vertebral bone marrow fat using chemical shift-encoding based water-fat MRI. Journal of magnetic resonance imaging : JMRI. 2015; 42(4):1018–1023. [PubMed: 25639780]
15. Loughran T, Higgins DM, McCallum M, Coombs A, Straub V, Hollingsworth KG. Improving highly accelerated fat fraction measurements for clinical trials in muscular dystrophy: origin and quantitative effect of R2* changes. Radiology. 2015; 275(2):570–578. [PubMed: 25575118]
16. Wang Z, Jiang T, Li J, et al. Regulation of renal lipid metabolism, lipid accumulation, and glomerulosclerosis in FVBdb/db mice with type 2 diabetes. Diabetes. 2005; 54(8):2328–2335. [PubMed: 16046298]
17. Mishra R, Emancipator SN, Miller C, Kern T, Simonson MS. Adipose differentiation-related protein and regulators of lipid homeostasis identified by gene expression profiling in the murine db/db diabetic kidney. American journal of physiology Renal physiology. 2004; 286(5):F913–921. [PubMed: 15075187]
18. Bobulescu IA, Dubree M, Zhang J, McLeroy P, Moe OW. Effect of renal lipid accumulation on proximal tubule Na+/H+ exchange and ammonium secretion. American journal of physiology Renal physiology. 2008; 294(6):F1315–1322. [PubMed: 18417539]
19. Peng XG, Bai YY, Fang F, et al. Renal lipids and oxygenation in diabetic mice: noninvasive quantification with MR imaging. Radiology. 2013; 269(3):748–757. [PubMed: 23901127]

20. Hammer S, de Vries AP, de Heer P, et al. Metabolic imaging of human kidney triglyceride content: reproducibility of proton magnetic resonance spectroscopy. PloS one. 2013; 8(4):e62209. [PubMed: 23620813]
21. Sijens PE, Edens MA, Bakker SJ, Stolk RP. MRI-determined fat content of human liver, pancreas and kidney. World journal of gastroenterology. 2010; 16(16):1993–1998. [PubMed: 20419836]
22. Eggers H, Brendel B, Duijndam A, Herigault G. Dual-echo Dixon imaging with flexible choice of echo times. Magnetic resonance in medicine. 2011; 65(1):96–107. [PubMed: 20860006]
23. Yokoo T, Shiehmorteza M, Hamilton G, et al. Estimation of hepatic proton-density fat fraction by using MR imaging at 3.0 T. Radiology. 2011; 258(3):749–759. [PubMed: 21212366]
24. Reeder SB, Cruite I, Hamilton G, Sirlin CB. Quantitative assessment of liver fat with magnetic resonance imaging and spectroscopy. Journal of magnetic resonance imaging : JMRI. 2011; 34(4): 729–749. [PubMed: 21928307]
25. Saaddine JB, Fagot-Campagna A, Rolka D, et al. Distribution of HbA(1c) levels for children and young adults in the U.S.: Third National Health and Nutrition Examination Survey. Diabetes care. 2002; 25(8):1326–1330. [PubMed: 12145229]
26. Druilhet RE, Overturf ML, Kirkendall WM. Structure of Neutral Glycerides and Phosphoglycerides of Human Kidney. Int J Biochem. 1975; 6(12):893–901.
27. de Vries AP, Ruggenenti P, Ruan XZ, et al. Fatty kidney: emerging role of ectopic lipid in obesity-related renal disease. The lancet Diabetes & endocrinology. 2014; 2(5):417–426. [PubMed: 24795255]
28. Kiss E, Kranzlin B, Wagenblabeta K, et al. Lipid droplet accumulation is associated with an increase in hyperglycemia-induced renal damage: prevention by liver X receptors. The American journal of pathology. 2013; 182(3):727–741. [PubMed: 23318573]
29. Yuan, Q.; Dimitrov, I.; Maalouf, NM.; Sakhaee, K.; Weatherall, PT. Spectroscopic Water-Fat Quantification in Human Kidney at 3T. ISMRM 19th Annual Meeting & Exhibition; Montreal, Canada. 2011; p. 871
30. Szczepaniak LS, Nurenberg P, Leonard D, et al. Magnetic resonance spectroscopy to measure hepatic triglyceride content: prevalence of hepatic steatosis in the general population. American journal of physiology Endocrinology and metabolism. 2005; 288(2):E462–468. [PubMed: 15339742]
31. Tang A, Desai A, Hamilton G, et al. Accuracy of MR imaging-estimated proton density fat fraction for classification of dichotomized histologic steatosis grades in nonalcoholic fatty liver disease. Radiology. 2015; 274(2):416–425. [PubMed: 25247408]
32. Pan LL, Zhang HJ, Huang ZF, et al. Intrahepatic triglyceride content is independently associated with chronic kidney disease in obese adults: A cross-sectional study. Metabolism: clinical and experimental. 2015; 64(9):1077–1085. [PubMed: 26144271]
33. Musso G, Gambino R, Tabibian JH, et al. Association of non-alcoholic fatty liver disease with chronic kidney disease: a systematic review and meta-analysis. PLoS medicine. 2014; 11(7):e1001680. [PubMed: 25050550]
34. Kuhn JP, Hernando D, Mensel B, et al. Quantitative chemical shift-encoded MRI is an accurate method to quantify hepatic steatosis. Journal of magnetic resonance imaging : JMRI. 2014; 39(6): 1494–1501. [PubMed: 24123655]
35. Tang A, Tan J, Sun M, et al. Nonalcoholic fatty liver disease: MR imaging of liver proton density fat fraction to assess hepatic steatosis. Radiology. 2013; 267(2):422–431. [PubMed: 23382291]
36. Yokoo T, Bydder M, Hamilton G, et al. Nonalcoholic fatty liver disease: diagnostic and fat-grading accuracy of low-flip-angle multiecho gradient-recalled-echo MR imaging at 1.5 T. Radiology. 2009; 251(1):67–76. [PubMed: 19221054]
37. Liu CY, McKenzie CA, Yu H, Brittain JH, Reeder SB. Fat quantification with IDEAL gradient echo imaging: correction of bias from T(1) and noise. Magnetic resonance in medicine. 2007; 58(2):354–364. [PubMed: 17654578]
38. Hernando, D.; Bashir, MR.; Hamilton, G., et al. Multi-Site, Multi-Vendor Validation of Accuracy, Robustness and Reproducibility of Fat Quantification on an Oil-Water Phantom at 1.5T and 3T. ISMRM 23rd Annual Meeding & Exhibition; Toronto, Canada. 2015; p. 0086

39. Mashhood A, Railkar R, Yokoo T, et al. Reproducibility of hepatic fat fraction measurement by magnetic resonance imaging. Journal of magnetic resonance imaging. JMRI. 2013; 37(6):1359–1370. [PubMed: 23172799]

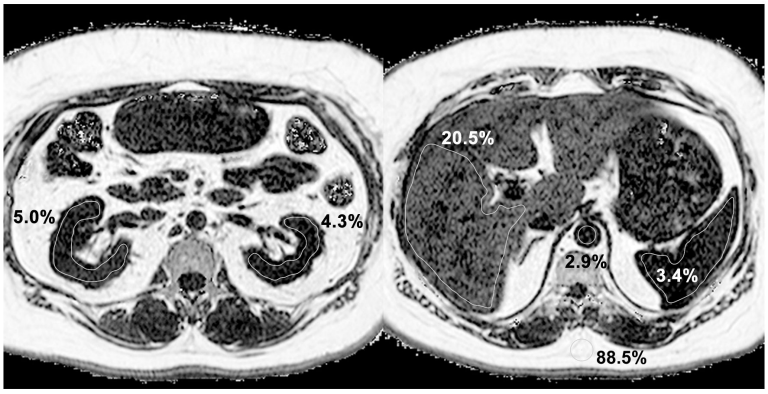

Figure 1.

An illustrative case

53-year old female with a history of type II diabetes mellitus. Two axial sections of the proton-density fat fraction (FF) maps are shown, mid abdomen at the level of the kidneys (left) and upper abdomen at the level of the liver and spleen (right). Typical region of interest (ROI) placement in the kidneys, liver, and spleen are illustrated. Both kidneys demonstrate higher than expected FF values in the inter-polar region (left). Hepatic FF is elevated (right) compatible with steatosis, whereas spleen and aorta are similar and lower in FF values. Subcutaneous fat shows expected FF value of ~90%. The pixel intensity range of 0-100% is displayed using a logarithmic scale to accentuate contrast in the low FF range.

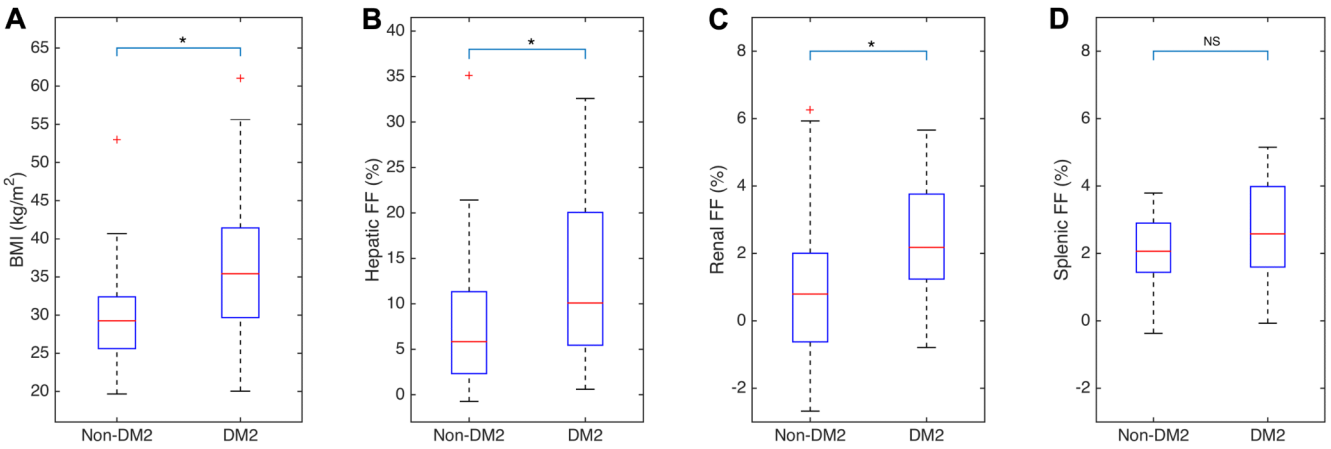

Figure 2.

Effects of diabetes on the BMI, hepatic FF, renal FF, and splenic FF

Legends: BMI = body mass index, FF = proton-density fat fraction, DM2 = type II diabetes mellitus. Asterisk (*) indicates statistically significant difference between the DM2 and non-DM2 cohorts, $p<0.05$ (see table 2), NS = not significant.

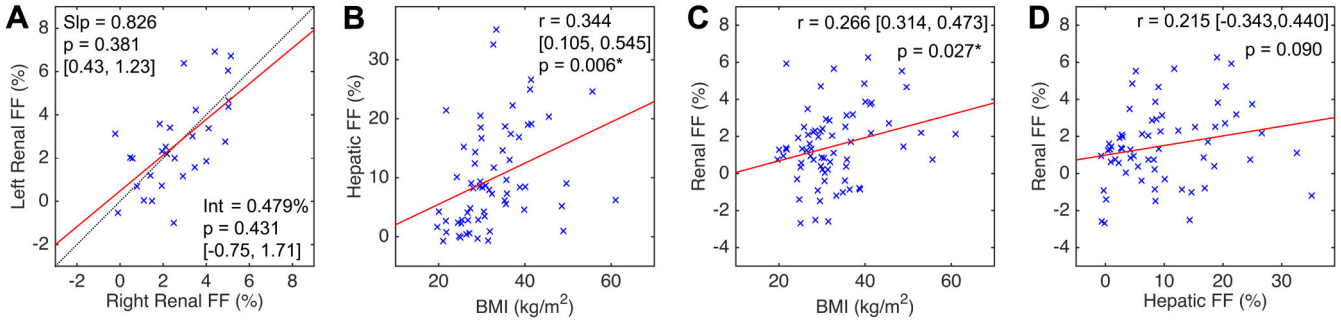

Figure 3.

Linear regression analysis [A] between right and left renal FF, [B] hepatic FF and BMI, [C] renal FF and BMI, and [D] renal and hepatic FF. Legends: Slp = slope, Int = intercept, and [,] = 95% confidence interval. FF = proton-density fat fraction, BMI – body mass index, r – Pearson's correlation coefficient. Asterisk (*) indicates statistical significance (p-value < 0.05).

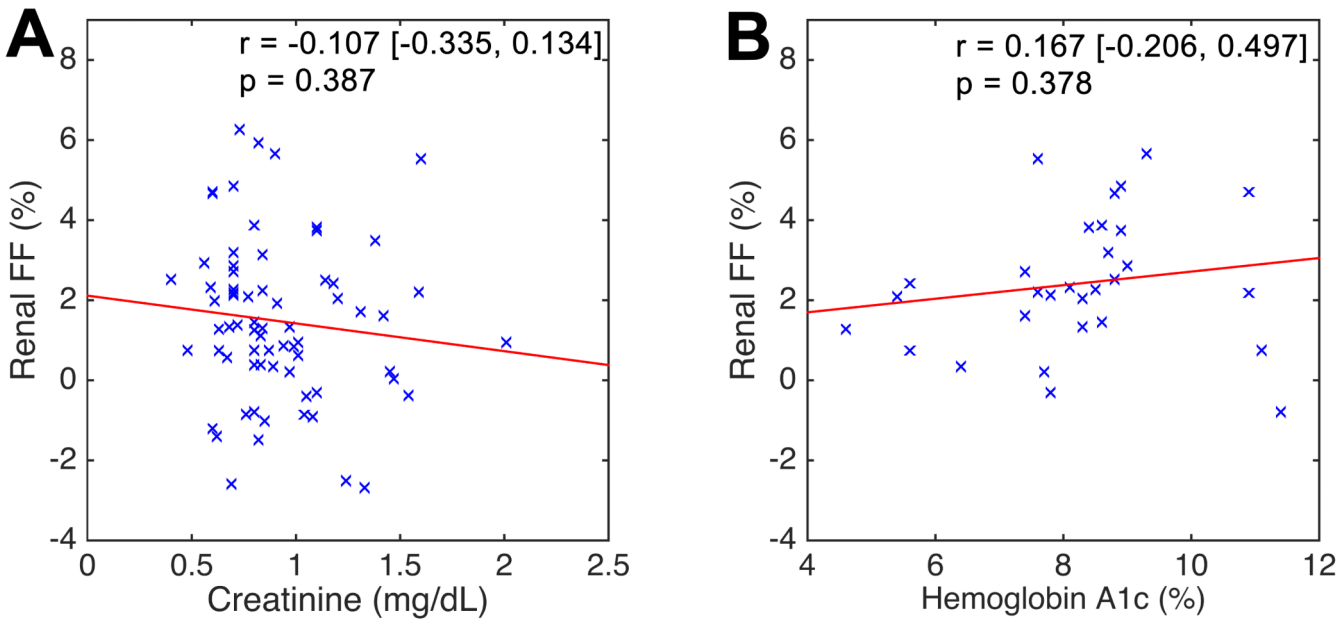

Figure 4.

Linear regression analysis between renal FF and [A] serum creatinine and [B] serum hemoglobin A1c (HbA1c). While serum creatinine levels were available for all subjects, measured HbA1c levels were only available in subjects with DM2. Legends: FF - proton-density fat fraction, r – Pearson's correlation coefficient. [,] = 95% confidence interval.

Table 1

Main inclusion and exclusion criteria for the study participants

Study	Inclusion Criteria	Exclusion Criteria
1	• Renal cancer > 2 cm in size with planned surgical resection	• Chronic renal insufficiency with eGFR <30 mL/min/1.73m^2
2	• Locally advanced or metastatic pancreas cancer on chemotherapy • ECOG functional status 0-2	• Prior radiation therapy for pancreas cancer • New chemotherapy initiated <14 days • Thiazolidinedione use within 12 months • History of HIV infection • Others * (ref - NCT01838317)
3	• History of DM2 • Insulin >1.5 units/kg/day • HbA1c 7.5 – 11% • Stable comorbidities, treatment regimen, oral hypoglycemics	• Type 1 diabetes mellitus • History of other pancreatic disease • End stage renal disease • Current use of steroid or incretin therapy • Others * (ref - NCT01505673)
All	• Age >18 years • Able to provide informed consent • Physically able to tolerate MRI • mDixon-Quant sequence performed	• Contraindicaition to MRI • Pregnant or lactating women • Claustrophobia • Weight > 400 lbs

Legends: ECOG – Eastern Cooperative Oncology Group; DM2 – type 2 diabetes mellitus; eGFR = estimated glomerular filtration rate; NYHA – New York Heart Association;

* other exclusion criteria unrelated to glucose or lipid metabolism detailed in http://www.clinicaltrials.gov under referenced identifier.

Table 2

Characteristics of the study population, grouped by diabetes status

	Combined	Non-DM2	DM2	Non-DM2 vs. DM2
Subjects (N)	69	40	29	–
Age (yrs)	58.0 ± 14.3	60.5 ± 18.0	55.0 ± 9.7	p=0.0896
Sex (M/F)	45/24	29/11	16/13	p=0.1358
BMI (kg/m^2)	30.6 ± 9.5	29.3 ± 6.8	35.4 ± 11.8	**p=0.0007**
Cr (mg/dL)	0.83 ± 0.39	0.85 ± 0.37	0.80 ± 0.33	p = 0.1545
HbA1c (%)	–	–	8.35 ± 1.30	–
Hepatic FF (%)	8.37 ± 13.47	5.83 ± 9.01	10.09 ± 14.61	**p=0.0117**
Renal FF (%)	1.33 ± 2.20	0.79 ± 2.63	2.18 ± 2.52	**p=0.0008**
Splenic FF (%)	2.16 ± 1.73	2.07 ± 1.46	2.58 ± 2.39	p=0.0923

Legends: FF – fat fraction; DM2 – type 2 diabetes mellitus; BMI – body mass index; Cr – serum creatinine; HbA1c – serum hemoglobin A1c. Median and ± interquartile range are reported for age, sex, BMI, creatinine, HbA1c, and FFs. Statistically significant p-values are shown in bold typeset.

Table 3

Multivariate Regression Analysis for Reanl FF

	Coefficient	Standard Error	*t*-statistic	p-value
Intercept	−1.4615	1.9255	−0.7590	0.4510
Age (yrs)	0.0378	0.0256	1.4763	0.1453
Sex (0,1)	−0.1357	0.5669	−0.2394	0.8117
BMI (kg/m^2)	0.0162	0.0341	0.4764	0.6356
Cr (%)	−1.7350	0.9148	−0.8034	0.4251
DM2 (0,1)	**1.7104**	**0.5800**	**2.9489**	**0.0045**
Hepatic FF (%)	0.0231	0.0310	0.7438	0.4601

Model: Renal FF ~ Intercept + Age + Sex + BMI + DM2 + Hepatic FF. Legends: Sex (0-male, 1-female); BMI – body mass index; Cr – serum creatinine; DM2 - type II diabetes mellitus (0-absent, 1-present); FF – proton-density fat fraction. Bold typeset indicates statistically significant p-value.